



A neuro-fuzzy approach to estimate the shear contribution of externally bonded FRP composites

Swapnasarit Kar¹ · A. R. Pandit¹ · K. C. Biswal¹

Received: 1 July 2020 / Accepted: 26 October 2020 / Published online: 16 November 2020
© Springer Nature Switzerland AG 2020

Abstract

The wide usage of fiber-reinforced polymer (FRP) composites as an external shear strengthening material have resulted in the development of various design guidelines. However, the accuracy of the design guidelines is a matter of concern since the shear behavior of the RC beam becomes more complex with the addition of FRP composites. On the other side, soft computing methods have been proved to be efficient enough to analyze complex systems. However, their application in structural engineering is limited. Therefore, in the current investigation, an effort has been made to evaluate the shear contribution of the EB-FRP composites with the help of adaptive neuro-fuzzy inference system (ANFIS). A total of 151 sets of data assembled from literature was utilized for the development and evaluation of the ANFIS model. The ANFIS predictions were validated against the obtained experimental results as well as with the estimations of six widely implemented design guidelines. The comparative study has shown that the ANFIS estimates are in decent agreement with that of experimental outcomes and the accurateness of the current ANFIS model is superior to the considered design guidelines. Finally, a parametric investigation was performed to explore the combined effect of various parameters as well as the impact of independent parameters.

Keywords RC beam · ANFIS · FRP · Shear strengthening · Shear contribution

List of symbols

A_f	Area of the FRP reinforcement and $A_f = 2nt_f w_f$	k_2	Modification factor applied to k_v to account for wrapping scheme
b_w	Width of the RC beam	L_e	Effective bond length
d	Effective depth of RC T-beam	n	Number of FRP layers
d_0	Distance of extreme compression fiber from the centroid of the outermost layer of tensile reinforcements	s_f	Center to center spacing of FRP strips
d_f	Effective depth of FRP	p_f	Spacing of FRP strips, measured orthogonally to the fiber direction
d_v	Effective depth in the CSA guidelines, maximum of $0.9d$ or $0.72 \times$ overall depth of RC beam	t_f	Thickness of FRP strip/sheet per layer
E_f	Elastic modulus of FRP (MPa) (in GPa for fib)	w_f	Width of FRP strip/sheet
f_{fd}/f_{fe}	Design strength/effective design strength of FRP	z	Internal lever arm
f_c	Mean cylindrical compressive strength of concrete, as specified in the original article	α	Angle in between principal fibers of FRP and the line perpendicular to the longitudinal axis of the member
f_{ctm}	Mean tensile strength of concrete	β	Angle in between the longitudinal axis of the beam and principal fiber direction
K_{EN}	Covering coefficient	$\epsilon_{f,e}/\epsilon_{fu}$	Effective/ultimate strain of FRP
k_v	Bond-reduction coefficient	τ_{max}	Maximum bond strength
k_1	Modification factor applied to k_v to account for concrete strength	θ	Inclination of critical shear crack (assumed equal to 45°)
		ρ_f	FRP reinforcement ratio and $\rho_f = A_f/b s_f$

✉ Swapnasarit Kar
514ce1019@nitrrkl.ac.in

¹ Department of Civil Engineering, National Institute of Technology Rourkela, Rourkela, Odisha, India

Introduction

The fiber-reinforced polymer (FRP) has been extensively used in the field of construction for the strengthening or rehabilitation of the reinforced concrete (RC) structures owing to their various benefits like high specific strength, superior corrosion resistance, ease of handling, ability to get along with different forms, and minimal variation to the cross-section characteristics and to the dead load of the RC structures (Kar and Biswal 2020a; Kibria et al. 2020). The rehabilitation of RC members can be done with different FRP systems such as wet layup systems (on-site impregnation and application of dry fiber fabrics or sheets), pre-cured systems (use of FRP composites that are manufactured off-site) and pre-preg systems (application of partially cured fiber fabrics or sheets). However, the desired FRP system should be chosen depending upon the structural requirements as well as the ease and simplicity of application ACI 440.2 R-17 (2017).

The RC beam predominantly either fails in flexure mode or shear mode. However, the flexural failure mode is wished as it permits redistribution of stress and provides forewarnings to inhabitants, while the shear failure is sudden and cataclysmic. Therefore, the RC beams with or without external strengthening schemes should have enough shear capacity to avoid shear failure. Over the past 30 years, countless researchers have explored the ability of externally bonded FRP (EB-FRP) composite for the performance enhancement of the shear deficient RC flexural members and the amount of studies is growing with time. Although these studies have shown that the EB-FRP composites have enhanced the performance of shear deficient RC specimens, the degree of effectiveness of EB-FRP composites depends on several factors, like concrete strength of RC beam (f_c), shear span to effective depth ratio (a/d), depth of FRP composites, thickness (t_f) and amount of FRP, nature of fiber, etc.

The shear response of a normal RC beam is a complicated matter. Thus, the available design guidelines have proposed methods based on either semi-empirical or empirical approaches to envisage the shear capacity of RC specimens. As the utilization of EB-FRP composite for shear rehabilitation of RC specimens is growing with time, several authors have proposed various theoretical models for the estimation of the shear capacity of RC beams rehabilitated with the EB-FRP composites (Chen and Teng 2003; Khalifa et al. 1998; Mofidi and Chaalal 2011; Triantafillou 1998). These models are predominantly grounded on the experimental observations and have followed a similar approach, which has been adopted for the standard RC beam. Based on the observations made from the experimental researches and analytical works,

several countries have developed design guidelines that elaborate on the comprehensive design processes for the implementation and the application of EB-FRP composites along with the quality control (ACI 440.2.R-17 2017; AS 5100.8 2017; CSA S806-12 2012; EN 1998-3:2005 2005; fib-TG 9.3 2001; TR 55 2012). However, the accuracy of the available design guidelines is limited due to the lack of consideration of several vital parameters, that could noticeably affect the involvement of EB-FRP composites. For instance, the available design guidelines have ignored the impact of a/d ratio on the shear contribution of EB-FRP composites. Besides this, they also ignored the impact of the width of the beam and the interrelation between the steel reinforcements and EB-FRP composites. Thus, there is a need for a more precise and reliable method to find out the extent of the involvement of EB-FRP composites in the shear resisting mechanism of the rehabilitated specimens, and this will eventually help in the more effectual use of FRP composites.

On the other hand, the soft computing (SC) method offers solutions with satisfactory accuracy for various complex problems, which may be either time-consuming or arduous to solve with the help of present knowledge. The artificial neural network (ANN) and fuzzy inference system (FIS) are regarded as two main branches of the SC method. The FIS is established on the proficiency of human reasoning and works through a rule-base to predict the fuzzy output of a complex method under consideration (Naderpour and Mirrashid 2020). The “fuzzy logic method” was initially introduced as a “fuzzy set theory” by Zadeh (1965). The “fuzzy set theory” permits smooth and progressive transaction from “belong to a set” to “not belong to a set” through membership functions (MFs). The MF allows users to transmit the uncertainty in the human awareness to the machine as well as to model various linguistic expressions such as “the speed is low,” “the room temperature is high,” etc. Although the implementation of FIS is an easy process, the selection of the shape of MFs as well as defining them for various input parameters require a considerable amount of time. Besides this, describing the degree of overlapping of MFs and their optimization depends on the human expertise in the understanding of the problem from various aspects.

On the other hand, ANNs are powerful computational models with efficient learning and adaption process. ANNs comprise a set of interrelated nodes and are motivated by the model of “the neurons in the brain” and change their structure in accordance with the flow of the information in the course of learning. The ANN models have been used in the broad spectrum of engineering applications due to its efficient learning and adaptation process, especially for complex systems. However, it is strenuous to explore the trained networks of ANNs, and the training process of the ANNs are moderately sluggish. Therefore,

to overcome these individual difficulties, the SC models can be combined to generate a hybrid and more efficient models such as ANFIS (adaptive neuro FIS). The ANFIS is a synergy of FIS and ANN, that wisely considers the strengths and eradicates the limitations of the FIS and ANN. The ANFIS represents a useful and smart method, which has the decision-making capacity of FIS and the learning ability of ANN. Therefore, it can be said that ANFIS is a FIS, which is employed in the framework of ANN. In recent years, the applications of different soft computing methods in various fields of engineering have increased significantly (Badaoui et al. 2019; Badawy 2020; Golnargesi et al. 2018; Kawady et al. 2020; Nguyen et al. 2020). However, the employment of these soft computing tools (SCTs) in the field of structural engineering is somewhat new.

Safa et al. (2016) investigated the ability of ANFIS in the prediction of shear capacity of RC beams. Jalal et al. (2020) presented an ANFIS model to estimate the compressive strength of rubberized concrete containing various proportions of zeolite, rubber chips and silica fume. Shariati et al. (2020) have employed ANFIS to find the parameters, which have a substantial effect on the actions of the pre-damaged RC beams. Naderpour and Mirrashid (2020) have estimated the moment capacity of RC columns using various soft computing tools and established that the ability of ANFIS is higher than the other considered soft computing tools. Naderpour and Alavi (2017), Kar and Biswal (2020b) and Kar et al. (2020) examined the viability of the ANFIS for the evaluation of the contribution of EB-FRP composites towards the shear capacity of rehabilitated RC specimens. Sharifi et al. (2019) established an ANN model for the assessment of the lateral-torsional buckling strength of the I-beams.

It has been perceived from the literature that the application of SCTs in the field of rehabilitation of RC flexural members with EB-FRP composites is limited. Hence, the authors have attempted to reconnoiter the applicability of the ANFIS for the calculation of the EB-FRP's shear contribution. In the current study, a database containing the outcomes of 151 shear rehabilitated RC beams was considered for the generation and assessment of the ANFIS model. The accurateness of the generated ANFIS model was validated against the experimentally observed shear contribution of EB-FRP composites. Besides this, the accurateness of the ANFIS model was also equated with the available design guidelines by means of different statistical measures. In addition to these, a parametric investigation was executed to assess the interactions of the various input parameters on the contribution of EB-FRP composites. At last, a detailed description of the considered ANFIS model with the help of a numerical example has been presented in this study.

Experimental database

It is significantly essential to have a database with similar kinds of data to generate an ANFIS model with adequate accuracy and reliability. Therefore, through a comprehensive review of available literature, 151 sets of data based on the RC specimens rehabilitated in shear with side-bonded (SB) FRP composites were accumulated (Adhikary and Mutsuyoshi 2004; Al-Akhras et al. 2016; Al-Sulaimani et al. 1994; Alam and Riyami 2018; Allam and Ebeido 2003; Azam et al. 2017; Barros and Dias 2003; Beber and Campos 2005; Bukhari et al. 2010; Bukhari et al. 2013; Chaallal et al. 1998; Ebead and Saeed 2017; Farghal 2012; Grande et al. 2009; Khalifa and Nanni 2000; Li et al. 2001; Lim 2010; Monti and Liotta 2007; Mostofinejad et al. 2016; Nikopour and Nehdi 2011; Norris et al. 1997; Obaidat et al. 2011; Panda et al. 2011, 2013a, b; Panigrahi et al. 2014; Panjehpour et al. 2014; Pellegrino and Modena 2002; Pham and Hao 2016; Tetta et al. 2015; Triantafillou 1998; Zhang et al. 2004; Zhang and Hsu 2005). In the SB scheme, the FRP sheets/strips are only glued to the web portion of the RC specimens with a bonding agent. Thus, the side-bonding scheme is the simplest shear strengthening scheme (Kar and Biswal 2020c). However, the current database has excluded the RC beams that have failed in flexure. The current database incorporates various parameters such as web width of RC beams (b_w), effective depth of FRP composites (d_f), a/d ratio, internal transverse reinforcement ratio (ρ_{sv}), f_c , experimentally observed shear contribution of EB-FRP composites (V_f). The V_f was enumerated by debiting the shear capacity of the control specimen (specimen without EB-FRP composites) from the failure load of FRP strengthened RC specimen. On the other hand, the ' d_f ' is deduced as the depth from the topmost edge of EB-FRP sheets/strips to the centroid of the bottom longitudinal steel reinforcements. Besides the above-mentioned data, the database also incorporates the overall thickness of FRP fabric/plates (product of the number of layers (n) and thickness of individual FRP layer (t_f)), center-to-center spacing (s_f) and width (w_f) of FRP strips, fiber orientation (β), modulus of elasticity (E_f) and ultimate strain (ϵ_{fu}) of FRP material. Table 1 gives a summary of the accumulated datasets.

ANFIS model

Jang combined the fuzzy logic and artificial neural network to introduce the ANFIS in 1993 and has developed a Sugeno type FIS (Jang 1993). In the 1st segment of the

Table 1 Statistical overview of the accumulated datasets

	b_w (mm)	d_f (mm)	a/d	f_c (MPa)	ρ_{sv} (%)	E_f (GPa)	$n \times t_f$ (mm)	W_f/S_f	ϵ_{fu} (%)	V_f (kN)
Minimum	70.00	90.00	1.00	11.21	0.00	6.83	0.095	0.13	0.60	1.00
Maximum	250.00	390.00	4.00	61.00	0.43	392.00	6.00	1.00	2.53	121.85
Mean	141.69	204.10	2.73	36.17	0.09	175.75	0.74	0.70	1.41	35.86
SD	41.06	70.11	0.56	9.77	0.13	103.53	0.80	0.30	0.36	21.88
Range	180.00	300.00	3.00	49.79	0.43	385.17	5.905	0.87	1.93	120.85
CoV	0.29	0.34	0.20	0.27	1.39	0.59	1.08	0.42	0.26	0.61

ANFIS model, a rule base comprising of fuzzy IF–THEN rules is created according to the assembled input and output data of the system under analysis. On the other hand, in the 2nd segment, these rules are adjusted by the neural network (NN) to achieve the best or intended ANFIS model. It is comparatively easier to describe the parameters as well as optimizing the MFs in the ANFIS method since ANFIS is not established on the knowledge of the expert rather than the training of the data (Tan et al. 2017). Thus, The time required for recognizing rules and MFs, as well as calculating the appropriate size and optimum structure of the NN, could be shortened by means of ANFIS (Khoshnevisan et al. 2014).

Theoretical framework of ANFIS

To describe the theoretical framework of ANFIS, a 1st order Sugeno type fuzzy model with two fuzzy rules (originally recommended by Jang (Jang 1993)) is presented below for completeness:

Rule 1 : if x is A_1 and y is B_1 then $f_1 = p_1x + q_1y + r_1$ (1)

Rule 2 : if x is A_2 and y is B_2 then $f_2 = p_2x + q_2y + r_2$ (2)

where $(x$ and $y)$ are input parameters, and f_i is the output. On the other hand, p_i , q_i , and r_i are regarded as premise

parameters (PP). Similarly, A_i and B_i symbolize the MFs of x and y , respectively. Figure 1 illustrates the corresponding ANFIS architecture. The output of the i th node of the layer “1” is represented by “ $O_{1,i}$ ”.

Layer 1: In this layer, all nodes are adaptive nodes. The node functions of the i th node are characterized as:

$$O_{1,i} = \mu_{A_i}(x) \quad \text{for } i = 1, 2 \tag{3}$$

$$O_{1,i} = \mu_{B_{i-2}}(y) \quad \text{for } i = 3, 4 \tag{4}$$

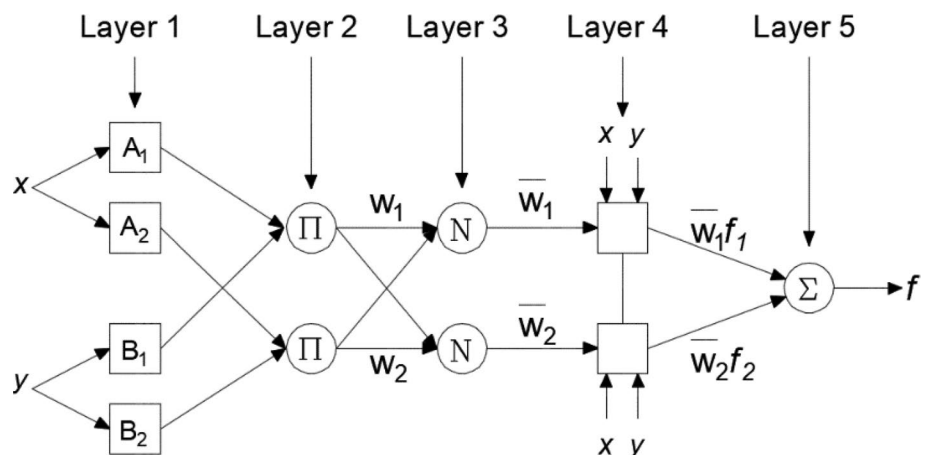
where, $O_{1,i}$ symbolizes the grade of MF of the fuzzy set. In addition, the $O_{1,i}$ designates the level of fulfilment of the quantifier, that can be satisfied by the corresponding input parameter. Based on the problem under evaluation, parameterized MFs such as Gaussian, bell, trapezoidal, triangular or any other profile can be considered as the MFs for both A_i and B_i .

Layer 2: Individual node in the current layer characterizes the firing strength (FS) of the rule. Therefore, this layer regulates the strength of rules. The output of this layer is described as:

$$O_{2,i} = w_i = \mu_{A_i}(x) \times \mu_{B_i}(y), \quad i = 1, 2 \tag{5}$$

Layer 3: Every node in the current layer computes the ratio of the FS of i th rule’s to the sum of FS of all the rules and is designated as:

Fig. 1 Architecture of ANFIS (Jang 1993)



$$O_{3,i} = \bar{w}_i = \frac{w_i}{w_1 + w_2}, \quad i = 1, 2 \quad (6)$$

Layer 4: The i th node estimates the involvement of the i th rule concerning the output, and is designated as:

$$O_{4,i} = \bar{w}_i f_i = \bar{w}_i (p_i x + q_i y + r_i), \quad \text{for } i = 1, 2 \quad (7)$$

where \bar{w}_i is the normalized FS as attained from the preceding layer, whereas the p_i , q_i and r_i are recognized as the consequent parameters and symbolize the optimal values, those are found at the end of the ANFIS training process.

Layer 5: This layer encompasses a lone node, which denotes the final output of the ANFIS model. The final output is the summation of all the signals coming from the preceding layer and is described as follows:

$$O_{5,1} = f = \sum \bar{w}_i f_i = \frac{\sum_i w_i f_i}{\sum_i w_i} \quad (8)$$

It is to be noted that in the ANFIS method, only the square nodes could be adjusted depending on the end user's necessities. The ANFIS model uses a hybrid learning algorithm (HLA), which is a conjunction of the backpropagation algorithm and the least square error (LSE) method to discover a likely set of the premise and consequent parameters. The HLA plunges convergence duration by decreasing the size of the search space of the backpropagation method (Jang 1993).

The preliminary FIS structure of the ANFIS model is either engendered by the subtractive clustering method or the grid partitioning method (GPM). In the GPM, a rule base is created by making an allowance for all the viable arrangements of various MFs for input parameters, which ultimately increases the dimensions of the rule base as well as the operation time. In contrast, the subtractive clustering method produces a rule base comparatively smaller than the rule base generated in the GPM since it is a one-pass algorithm (Vasileva-Stojanovska et al. 2015). Thus, the subtractive clustering method, as suggested by Chiu (1994), has been employed to describe the preliminary fuzzy model.

Proposed ANFIS model

The most important target of the present analysis is to consider all the key parameters, those could have a significant impact on the shear contribution of EB-FRP composites. Therefore, through the thorough analysis of different design guidelines, which are focused on the shear rehabilitation of RC specimens using EB-FRP composites and the observations made in different experimental studies, the parameters such as b_w , d_f , a/d , t_f , f_c , ε_{fu} , n , s_f , w_f , β and E_f have been considered as input parameters. However, to have an appropriate and competent soft computing

model with a comparatively lesser number of input parameters and reliable accuracy, several parameters have been combined with an aim to decrease the number of input parameters.

As per the formulations of different design guidelines, the V_f is directly proportional to the parameters such as n , t_f , E_f and w_f , whereas inversely proportional to the s_f . Therefore, n , t_f and E_f have been merged to generate a new parameter (M), as mentioned in Eq. (9). Similarly, the w_f and s_f , along with the orientation of fibers (β), have been amalgamated to produce a new parameter (N), as per the Eq. (10). The parameter “ M ” and “ N ” can adequately consider the variations in the FRP material properties and the type of strengthening schemes, respectively. Finally, b_w , d_f , a/d , f_c , ρ_{sv} , M , N and ε_{fu} have been considered as the input parameters, whereas the V_f is reckoned as the single output parameter. Figure 2 represents the summary of the input parameters along with the output parameter:

$$M = n \times t_f \times E_f \quad (9)$$

$$N = \frac{w_f}{s_f} \times (\sin\beta + \cos\beta) \quad (10)$$

It can be perceived from Fig. 2 that the input parameters have a very wide range of values. On the other hand, it is recommended to use a database with an equal range in each aspect of different input parameters for the development of an ANFIS model. A database with an equal range in each dimension will help in the acceleration of the ANFIS training process. Therefore, the input parameters have been normalized between 0.01 and 0.99 as follows:

$$IP_{i,norm} = 0.01 + 0.98 \times \frac{IP_i - IP_{min}}{IP_{max} - IP_{min}} \quad (11)$$

where, $IP_{i,norm}$, IP_i , IP_{min} , IP_{max} represents the normalized input value, actual input value, minimum and maximum input values for the corresponding input parameter, respectively.

After the completion of the normalization process of different input parameters, 121 sets of data (approximately 80%) were randomly selected from the whole dataset for the training of the ANFIS model, while the outstanding 30 sets of data were considered for the testing of the developed model. Among the various MFs, Gaussian MF has the most suitable characteristics to epitomize the real aspects of the different situations (Pandit et al. 2015; Tan et al. 2017). Also, the Gaussian MF is the most accurate MF to define the uncertainty in most of the real-life instances and also has the ability to approach the actual continual function on a compacted set with comparable accuracy (Kreinovich et al. 1992; Singh et al. 2013). Therefore, the Gaussian MFs (as described below) have been used in this investigation.

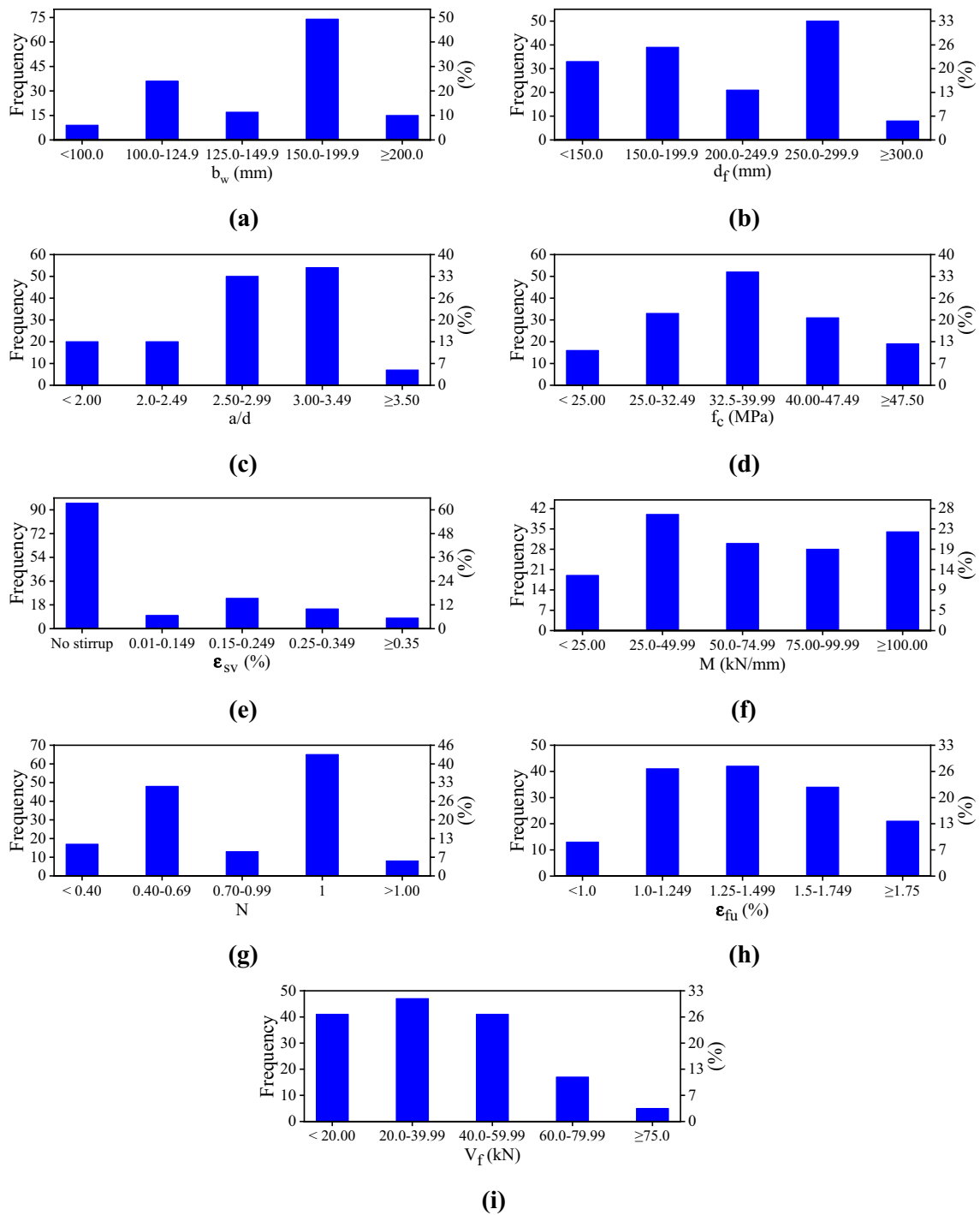


Fig. 2 Summary of the input and output parameter

$$\text{gaussian MF}(x, c_i, \sigma_i) = \exp\left(-\frac{1}{2}\left(\frac{x - c_i}{\sigma_i}\right)^2\right) \quad (12)$$

where c_i denotes the MF's center and σ_i signifies the width of the MF.

It is evident from the literature that the radius of the cluster center (r) considerably influences the number of rules to be created in the subtractive clustering method. Therefore, in the current study, several neuro-fuzzy models with different values of “ r ” were analyzed to find the best ANFIS model

Table 2 Performance of various ANFIS model

Model no.	<i>r</i>	No. of rules	Training dataset					Testing dataset					Whole dataset				
			Mean	CoV	R^2	MAPE	RMSE	Mean	CoV	R^2	MAPE	RMSE	Mean	CoV	R^2	MAPE	RMSE
			1	0.965	4	1.046	0.500	0.869	27.559	7.967	0.997	0.386	0.903	24.188	6.891	1.036	0.481
2	0.950	4	1.037	0.466	0.871	27.084	7.907	0.999	0.429	0.897	25.634	7.115	1.029	0.459	0.875	33.440	8.665
3	0.940	4	1.039	0.470	0.869	27.128	7.953	0.998	0.415	0.898	25.082	7.073	1.031	0.461	0.874	26.722	7.786
4	0.925	4	1.048	0.475	0.867	27.151	8.024	0.997	0.402	0.902	24.313	6.932	1.038	0.463	0.873	26.587	7.819
5	0.910	5	1.085	0.403	0.855	24.312	8.377	1.001	0.309	0.908	19.620	6.774	1.069	0.390	0.864	23.380	8.084
6	0.905	5	1.082	0.386	0.853	24.291	8.425	1.006	0.321	0.904	20.175	6.864	1.067	0.376	0.862	23.473	8.139
7	0.900	5	1.075	0.417	0.891	22.533	7.278	0.980	0.240	0.931	15.895	6.076	1.056	0.394	0.897	21.214	7.056
8	0.895	5	1.079	0.377	0.849	23.840	8.551	0.994	0.325	0.903	20.906	6.945	1.062	0.370	0.858	23.257	8.257
9	0.890	6	1.030	0.348	0.941	16.372	5.355	1.108	0.368	0.773	25.111	11.555	1.046	0.354	0.900	18.108	7.036
10	0.880	6	1.038	0.356	0.937	17.250	5.521	1.100	0.371	0.791	29.749	12.699	1.050	0.360	0.890	19.734	7.514
11	0.870	6	1.045	0.360	0.915	19.426	6.411	1.092	0.394	0.746	29.912	12.507	1.054	0.368	0.871	21.509	8.001
12	0.850	6	1.048	0.364	0.914	19.909	6.468	1.075	0.387	0.775	29.160	11.424	1.053	0.369	0.879	27.139	8.614
13	0.830	7	1.032	0.330	0.946	13.975	5.092	1.138	0.445	0.688	33.949	13.161	1.054	0.363	0.888	17.944	7.429
14	0.820	8	1.037	0.304	0.953	11.718	4.772	1.042	0.394	0.771	28.165	12.187	1.038	0.324	0.905	14.985	6.911
15	0.815	9	1.036	0.302	0.952	12.090	4.800	1.049	0.591	0.460	38.575	20.652	1.039	0.379	0.806	17.352	10.159
16	0.81	10	1.036	0.299	0.957	9.797	4.583	0.925	0.757	0.406	41.792	25.091	1.014	0.414	0.756	16.154	11.913
17	0.800	11	1.033	0.300	0.957	9.684	4.562	0.991	0.696	0.390	40.007	28.907	1.025	0.404	0.716	15.708	13.516

for the problem under consideration. Table 2 denotes the performance of some of the considered ANFIS models in terms of different statistical parameters (Eqs. 13–15):

$$\text{MAPE} = \frac{100}{n} \sum_{i=1}^n \left(\frac{|V_{f,ana} - V_{f,expt}|}{V_{f,expt}} \right) \quad (13)$$

$$R^2 = \frac{(n \sum (V_{f,expt} V_{f,ana}) - (\sum V_{f,expt})(\sum V_{f,ana}))^2}{[n \sum V_{f,expt}^2 - (\sum V_{f,expt})^2] - [n \sum V_{f,ana}^2 - (\sum V_{f,ana})^2]} \quad (14)$$

$$\text{RMSE} = \sqrt{\frac{1}{n} \sum_{i=1}^n (V_{f,ana} - V_{f,expt})^2} \quad (15)$$

By the comparison of different statistical parameters, as mentioned in Table 2, the best ANFIS model was chosen depending on the following criteria. A good ANFIS model should possess low CoV, RMSE and MAPE values for the whole set of data as well as the mean of the ratio estimated to investigational outcomes and R^2 closest to 1.0. In addition, the ANFIS model without considerable variation in the various statistical measures concerning the testing and training dataset should be preferred. On the other hand, it is inevitable to obtain two or more ANFIS models with similar performance. In this case, the ANFIS model with comparatively less number of rules should be preferred (Naderpour and Alavi 2017; Kar et al. 2020). Depending upon the criteria as discussed above, model no. 7 (Table 2) is selected for the current investigations. Figure 3 represents the MFs for various input parameters and Fig. 4 indicates the corresponding structure of the considered ANFIS model.

In this work, the selected ANFIS model has five fuzzy rules and they are described as follows:

Rule 1 : if X_1 is MF₁ and X_2 is MF₁ and X_3 is MF₁ and X_4 is MF₁ and X_5 is MF₁ and X_6 is MF₁ and X_7 is MF₁ and X_8 is MF₁ then Y is Z_1 .

Rule 2 : if X_1 is MF₂ and X_2 is MF₂ and X_3 is MF₂ and X_4 is MF₂ and X_5 is MF₂ and X_6 is MF₂ and X_7 is MF₂ and X_8 is MF₂ then Y is Z_2 .

Rule 3 : if X_1 is MF₃ and X_2 is MF₃ and X_3 is MF₃ and X_4 is MF₃ and X_5 is MF₃ and X_6 is MF₃ and X_7 is MF₃ and X_8 is MF₃ then Y is Z_3 .

Rule 4 : if X_1 is MF₄ and X_2 is MF₄ and X_3 is MF₄ and X_4 is MF₄ and X_5 is MF₄ and X_6 is MF₄ and X_7 is MF₄ and X_8 is MF₄ then Y is Z_4 .

Rule 5 : if X_1 is MF₅ and X_2 is MF₅ and X_3 is MF₅ and X_4 is MF₅ and X_5 is MF₅ and X_6 is MF₅ and X_7 is MF₅ and X_8 is MF₅ then Y is Z_5 .

where X_1, X_2, \dots, X_8 denotes the normalized values of input data. On the other hand, Z_1, Z_2, \dots, Z_5 are the linear functions of the input parameters, as outlined in Eq. (16).

$$Z_k = C_{0k} + C_{1k}X_1 + C_{2k}X_2 + C_{3k}X_3 + C_{4k}X_4 + C_{5k}X_5 + C_{6k}X_6 + C_{7k}X_7 + C_{8k}X_8 \quad (16)$$

where $C_{0k}, C_{1k}, C_{2k}, \dots, C_{8k}$ are the constants for the k th rule. Table 3 illustrates the constants of all the fuzzy rules of the current ANFIS model.

The outcome of the developed ANFIS model (V_f) is determined by the addition of outcomes of all the fuzzy rules, as represented in Eq. (17). The FIS diagram of the considered ANFIS model is illustrated in Fig. 5 for an input value (0.3911, 0.6535, 0.1728, 0.5181, 0.010, 0.0822, 0.6751, 0.4670).

$$V_{f,ANFIS} = \frac{\sum_{i=1}^k W_i Z_i}{\sum_{i=1}^k W_i} = \frac{w_1 Z_1 + w_2 Z_2 + w_3 Z_3 + w_4 Z_4 + w_5 Z_5}{w_1 + w_2 + w_3 + w_4 + w_5} \quad (17)$$

where w_1, w_2, w_3, w_4 and w_5 denote the weightage of rules 1, 2, 3, 4 and 5, respectively. Table 4 indicates the values of w_i, Z_i , and $w_i Z_i$ for the input vector, as mentioned above.

Overview of design guidelines

In recent years, a significant number of investigations have been performed to understand the behavior of shear deficient RC flexural specimens rehabilitated with EB-FRP

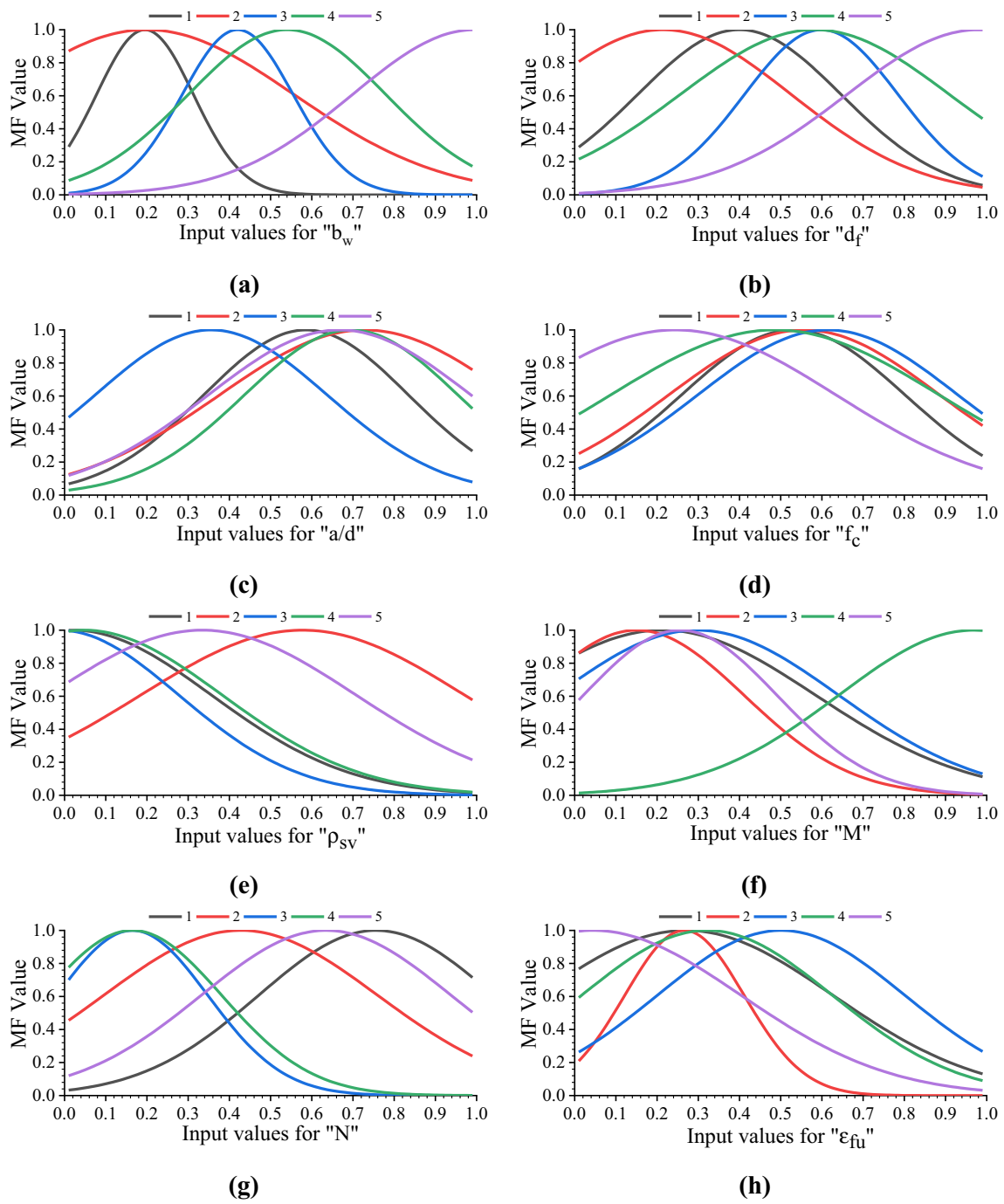


Fig. 3 MFs for different input parameters

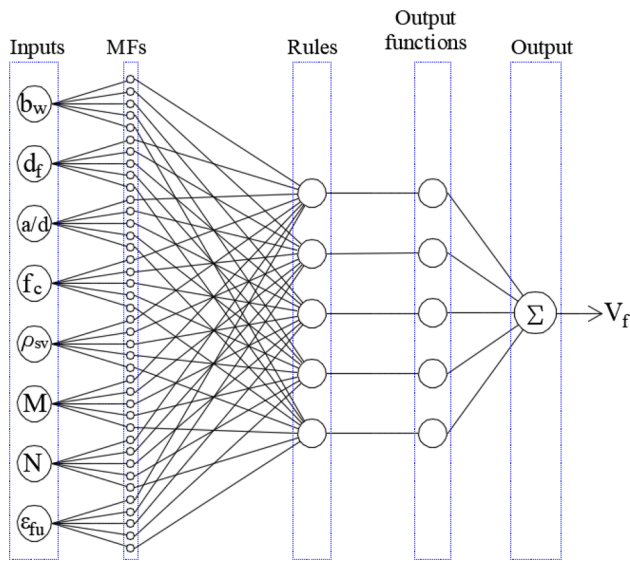


Fig. 4 Structure of the current ANFIS model

composites. These investigations have resulted in the development of several analytical models and design guidelines for RC flexural members rehabilitated in shear with EB-FRP composites. A summary of some of these guidelines for the estimation of shear resistance offered by side-bonded FRP composites is given below.

ACI 440.2 R-17

$$V_f = \frac{A_f f_{fe} (\sin\beta + \cos\beta) d_f}{s_f} \tag{18}$$

$$f_{fe} = \epsilon_{fe} E_f \tag{19}$$

where

$$\epsilon_{fe} = k_v \epsilon_{fu} \leq 0.004 \tag{20}$$

$$k_v = \frac{k_1 k_2 L_e}{11,900 \epsilon_{fu}} \leq 0.75 \tag{21}$$

Table 3 Linear co-efficient for different rules

Rule no.	C_0	C_1	C_2	C_3	C_4	C_5	C_6	C_7	C_8
1	-19.78	68.96	-45.77	26.44	107.5	167.7	30.23	-30.44	44.02
2	-48.31	0.3869	-7.335	18.22	8.979	16.6	12.11	-12.74	87.94
3	515.5	-957.6	184.7	74.94	45.24	215.1	-284.5	118	-370.5
4	79.8	733.8	-856.2	-376.6	-409.5	-33.24	441.6	35.02	291.1
5	-205.4	37.61	185.8	-53.81	48.88	-152.8	442	-6.854	136.7

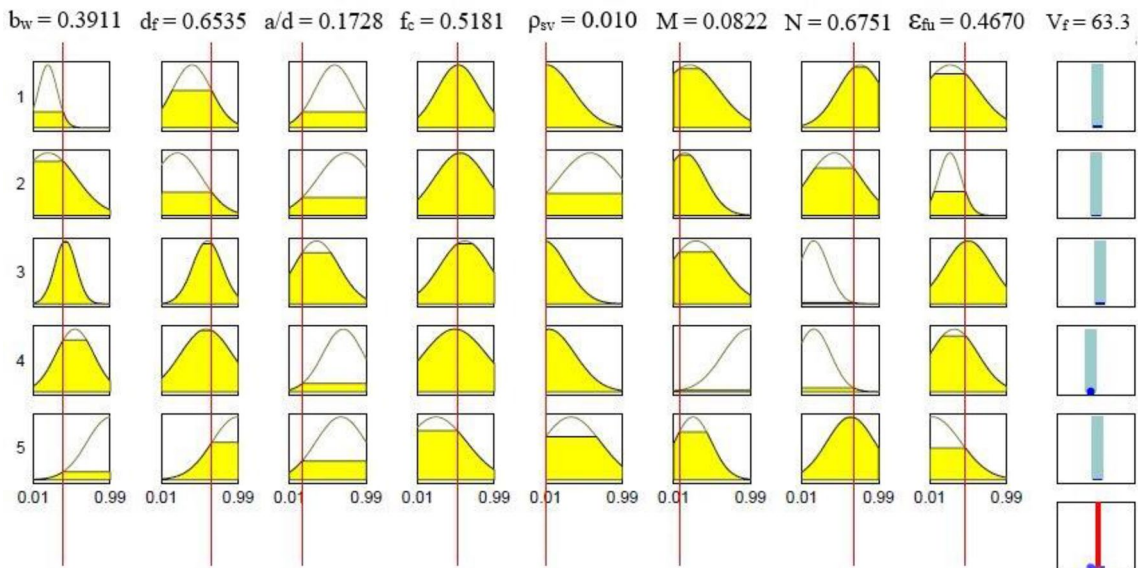


Fig. 5 FIS diagram of the present ANFIS model

Table 4 W_i and Z_i values for the considered input

w_i	Z_i	$w_i Z_i$	$w_i Z_i$	$w_i Z_i$
w_1	0.02877	Z_1	41.706	$w_1 Z_1$ 1.199
w_2	0.00911	Z_2	-11.524	$w_2 Z_2$ -0.105
w_3	0.01212	Z_3	183.474	$w_3 Z_3$ 2.223
w_4	0.00015	Z_4	-274.421	$w_4 Z_4$ -0.041
w_5	0.00456	Z_5	40.766	$w_5 Z_5$ 0.186

$$k_1 = \left(\frac{f_c}{27}\right)^{2/3}, \quad k_2 = \frac{d - 2L_e}{d_f}, \quad L_e = \frac{23,300}{(nt_f E_f)^{0.58}} \quad (22)$$

fib

$$V_f = 0.9 \epsilon_{fe} E_f \rho_f b_w d (\cot \theta + \cot \beta) \sin \beta \quad (23)$$

where

$$\epsilon_{fe} = \min \left\{ \begin{array}{l} 0.17 \left(\frac{f_c}{E_f \rho_f}\right)^{0.3} \epsilon_{fu} \text{ (fracture)} \\ 0.65 \left(\frac{f_c}{E_f \rho_f}\right)^{0.56} \times 10^{-3} \text{ (peeling-off)} \end{array} \right. \quad (24)$$

TR 55

$$V_f = \frac{2nt_f w_f}{s_f} \left(d_f - \frac{2L_e \cos \alpha}{3}\right) E_f \epsilon_{fe} (\sin \alpha + \cos \alpha) \quad (25)$$

where

$$\epsilon_{fe} = \min \left\{ 0.5 \epsilon_{fu}, 0.5 \sqrt{\frac{f_{ctm}}{E_f nt_f}}, 0.004 \right\} \quad (26)$$

$$L_e = 0.7 \sqrt{\frac{E_f nt_f}{f_{ctm}}} \quad (27)$$

EN 1998-3

$$V_f = 0.9 d f_{fe} 2nt_f \frac{\sin \beta}{\sin \theta} \frac{w_f}{p_f} \quad (28)$$

where

$$f_{fe} = f_{fd} \frac{z_{rid,eq}}{z} \left[1 - \sqrt{\frac{\pi - 2}{\pi} \frac{L_{eq}}{z_{rid,eq}}} \right]^2 \quad (29)$$

$$z_{rid,eq} = z_{rid} + L_{eq} \quad (30)$$

$$z_{rid} = z - L_e \sin \beta \quad (31)$$

$$L_{eq} = \frac{k_{EN} E_f \sin \beta}{3f_{fd}} \quad (32)$$

$$L_e = \sqrt{\frac{E_f nt_f}{\sqrt{4\tau_{max}}}} \quad (33)$$

$$f_{fd} = \sqrt{\frac{0.6 E_f f_{ctm} K_{EN}}{nt_f}} \quad (34)$$

$$K_{EN} = \sqrt{\frac{1.5(2 - w_f/p_f)}{1 + (w_f/100\text{mm})}} \quad (35)$$

$$\tau_{max} = 1.8 f_{ctm} K_{EN} \quad (36)$$

AS 5100.8

$$V_f = \frac{\epsilon_{fe} E_f A_f d_0 (\cot \theta + \cot \beta) \sin \beta}{S_f} \quad (37)$$

where

$$\epsilon_{fe} = k_v \epsilon_{fu} \leq 0.004 \quad (38)$$

$$k_v = \frac{k_1 k_2 L_e}{11900 \epsilon_{fu}} \leq 0.75 \quad (39)$$

CSA-S806

$$V_f = \frac{0.4 A_f f_{fe} d_v}{S_f} \cot \theta \quad (40)$$

where

$$f_{fe} = 0.005 E_f \quad (41)$$

It is to be noted that, the safety factors associated with the various design guidelines for the estimation of the V_f , have been taken as equal to 1.0. However, all other limitations, such as effective strain (ϵ_{fe}) have to be less than or equal to 0.004 (according to AS and ACI guidelines), will be taken into consideration for the evaluation of V_f . Besides these, the average concrete strength, as mentioned in the original articles, will be used for the calculation of different parameters as well as V_f .

Fig. 6 Comparison in between ANFIS forecasts and experimental outcomes

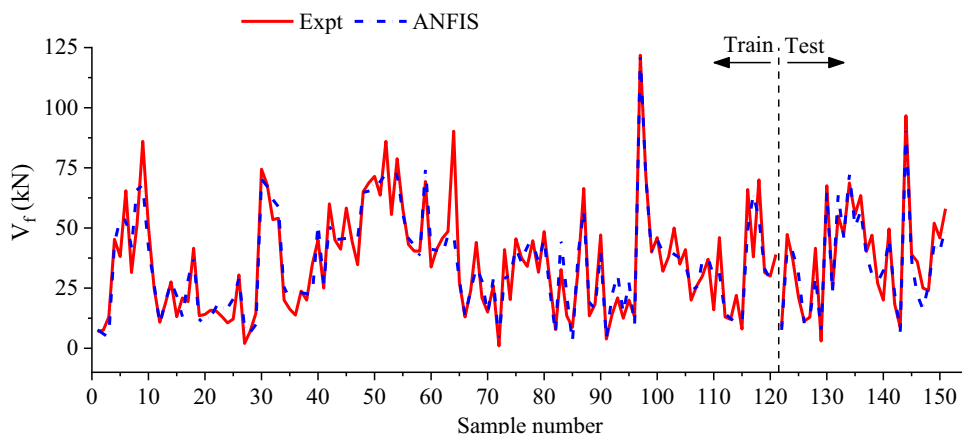


Table 5 Statistical evaluation of the ANFIS model and various design guidelines

Model	ANFIS	ACI	FIB	TR55	AS	EN	CSA
Mean	1.056	1.617	5.128	1.349	2.077	1.901	2.187
CoV	0.394	1.760	2.216	1.835	2.583	3.231	2.757
SD	0.416	2.847	11.363	2.475	5.366	6.141	6.030
R^2	0.897	0.269	0.202	0.275	0.229	0.109	0.128
MAPE	21.21	129.06	422.16	79.66	179.44	139.15	163.30
RMSE	7.056	50.089	118.297	29.003	55.416	25.808	47.065

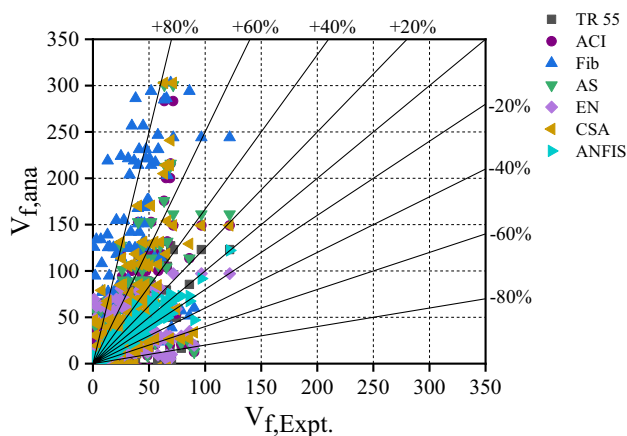


Fig. 7 Comparison between design guidelines and ANFIS

Results and discussions

Comparison between the experimental results and ANFIS model

In this section, the estimations produced by the developed ANFIS model ($V_{f,ANFIS}$) were linked with the experimental outcomes ($V_{f,Expt}$) through a one-to-one comparative study for the whole dataset. Figure 6 depicts the assessment of the predictions made by the present predictive model concerning

the investigational results. It can be deduced that the ANFIS estimations have a decent agreement with the experimental outcomes. However, small mismatches have been perceived for the training dataset along with the testing dataset, which could be due to the large variations in the considered datasets.

Comparison between the current ANFIS model and the design guidelines

In this section, the exactness of the current ANFIS model was weighed up with the design guidelines by means of different statistical measures and depicted in Table 5. A graphical comparative study between the forecasts of the current ANFIS model and various design guidelines is also presented in Fig. 7.

From Fig. 7, it could be visualized that a large portion of the ANFIS forecasts rests nearer to the unit slope line, especially between the +20 and –20%. In contrast, the forecasts made by guidelines are mostly disseminated, particularly above the unit slope line. The standard deviation (σ) and the mean of the $V_{f,ANFIS}/V_{f,Expt}$ are observed to be 0.416 and 1.056, respectively, Correspondingly, the MAPE, R^2 and RMSE are acquired to be 21.21, 0.897 and 7.056, respectively. Among the considered design guidelines, except the EN and CSA guidelines, all the guidelines have nearly the same R^2 values. On the other hand, the mean of

the predicted to experimentally obtained V_f and MAPE values are nearly similar for the AS and CSA guidelines. Even though the RMSE value for the TR 55 guideline is not the lowest amongst the design guidelines, the performance TR 55 guideline can be regarded to be slightly superior to the remaining ones due to the lowest mean, σ and MAPE values. Similarly, it can also be concluded that the predictions made by fib guidelines is not encouraging due to the very high values of different statistical parameters.

Parametric study

On the basis of the current ANFIS model, a brief discussion has been made on the collective influence of two separate parameters, as well as the influence of individual parameters on the V_f .

The ANFIS has the ability to represent the combined effect of two distinct parameters on the V_f through 3D-surface diagrams. It illustrates the collective impact of two distinguished parameters while the remaining input parameters remain unchanged and equal to the mid-value of the input dataset. To study the combined impact of different input parameters on the V_f of the current ANFIS model, a total of 28 number of surface diagrams were obtained. However, only some of them have been presented in Fig. 8.

In Fig. 8a, the combined effect of the b_w and d_f on the V_f is illustrated, whereas Fig. 8b signifies the combined effect of a/d ratio and d_f on the V_f . Likewise, Fig. 8c–f illustrates the combined consequence of (a/d and f_c), (f_c and ρ_{sv}), (M and N) and (N and b_w) on the V_f , respectively. From Fig. 8a it can be witnessed that the V_f followed an alternative increasing and decreasing trend with an increase in values of both b_w and d_f . It can be noted from Fig. 8b that, for lesser values of d_f , the V_f increases with an increase in a/d value and then decreases. On the other hand, for higher a/d ratios, the V_f first increases gradually with an increase in d_f values and then decreases up to some extent, after which it increases with a higher slope for an increase in d_f values. Similarly, the combined effect of other parameters can be analysed from Fig. 8.

On the other hand, the impact of the individual parameter was investigated by varying the considered parameter within 0.01–0.99 while keeping all others to a constant value and equal to the median value of the different input parameters. Figure 9 denotes the effect of various parameters on the V_f .

It can be observed from Fig. 9, the V_f gradually increases with an increase in b_w until 0.3 and then decreases until 0.6. However, the V_f again increases with an increase in b_w . It can be depicted that the V_f gradually increases with an increase in d_f values up to 0.7 and then decreases. For a/d value, the V_f increases with an increase

in a/d value till 0.4 and then reduces with an increase in a/d value. Similarly, for the most part of the concrete strength, it can be observed that the V_f increases with an increase in f_c . It can be noticed that steel stirrup has an adverse influence on the V_f . However, a slightly different trend has been observed for the lower as well as for higher values of ρ_{sv} . For M , the V_f decreases gradually with an increase in M up to 0.5 and then abruptly increases with M . On the other hand, the V_f increases with a stiffer slope for an increase in N until 0.3 and then it slowly increases with an increase in N values. For ε_{fu} greater than 0.5, the V_f decreases with a comparatively stiffer slope with an increase in ε_{fu} .

Conclusions

The current study has been primarily set out to explore the ANFIS model for the evaluation of the shear contribution of EB-FRP composites based on a database encompassing the outcomes of 151 experimental tests. The database was divided into 2 groups of 121 and 30 sets of data for the training and testing of the developed ANFIS model, respectively. Then, a comprehensive description of the considered predictive model was given with the help of an example for a deeper understanding of the fundamental mechanism of the ANFIS method. The ANFIS estimations were compared up against the experimental outcomes. The below-mentioned conclusions could be made from the present investigation:

1. It can be observed that there is an existence of a sound agreement amongst the ANFIS forecasts and the observed experimental results. The average of the ratio of the ANFIS forecasts to the experimentally found value was found to be approximately equal to one.
2. The effectiveness of the ANFIS model was related against the some of the available design guidelines through different statistical measures and it could be deduced that the efficacy of the ANFIS model was more than the considered design guidelines.
3. The estimations done by various design guidelines are observed to vary from the experimental ones significantly and some of the predictions are either too conservative or extremely over-estimated ones. However, the efficacy of the TR 55 guideline may be regarded as better than the other guidelines.
4. In addition to these, parametric inquiries were conducted to inspect the influence of different variable's on the ANFIS results. Unlike the analytical approaches, the ANFIS is capable to show the combined impact of two separate parameters, which could be used for the future improvement of the design guidelines.

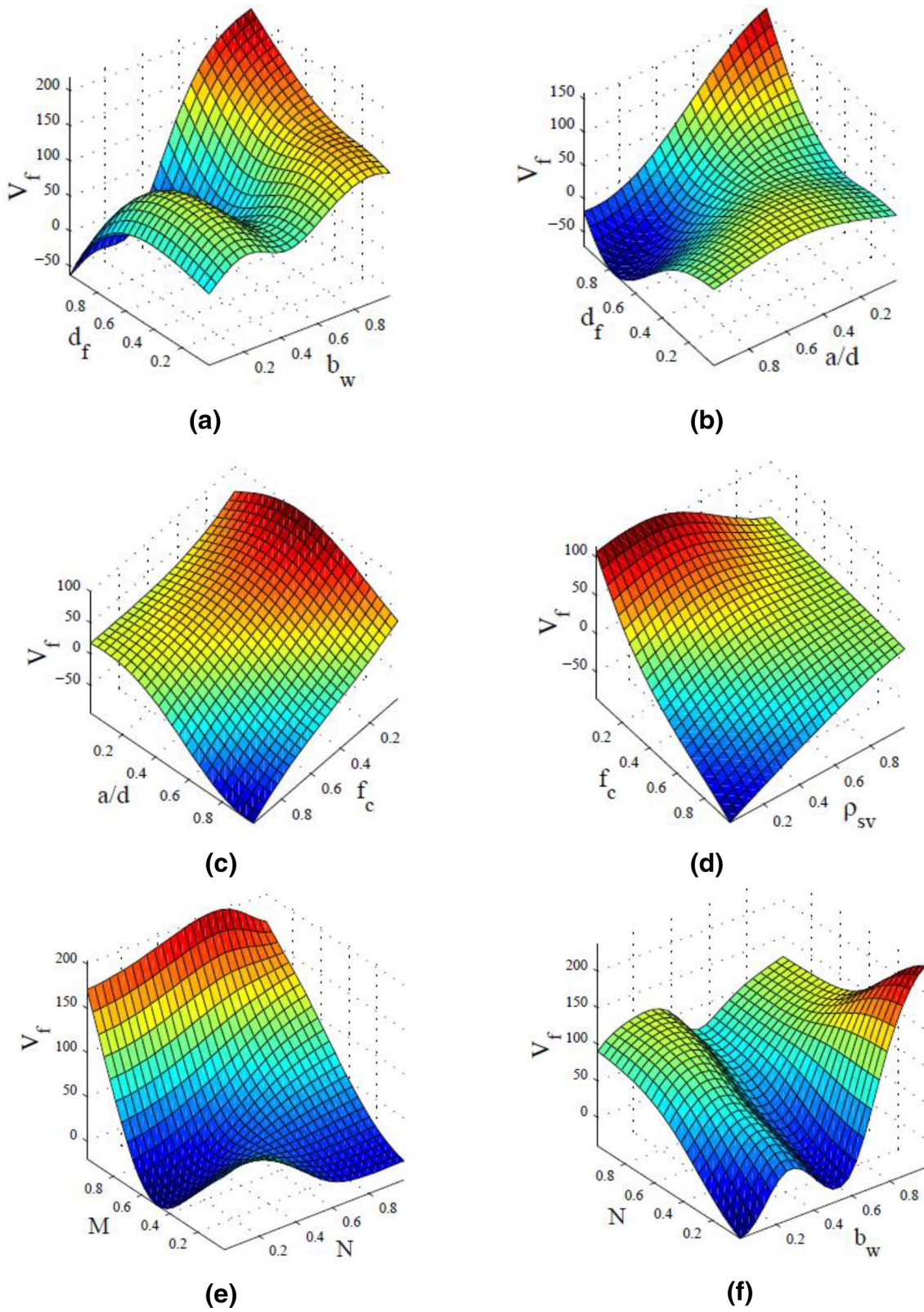


Fig. 8 Parametric study of the current ANFIS model for combinations of two input variables

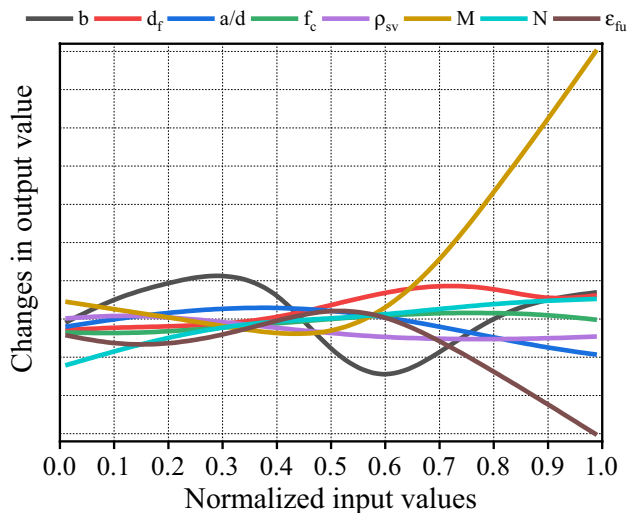


Fig. 9 Effect of individual parameters

5. The results of the present investigations have shown that the ANFIS tool can be reliably used as a probable alternative to the theoretical models for the shear contributions of the externally bonded FRP composites. It is to be noted that the present ANFIS model is developed within a set of data and can be modified further with the inclusion of more datasets in the near future. Thus, the effectiveness of the current ANFIS model may vary when utilized for the datasets lying outside the considered range.

Compliance with ethical standards

Conflict of interest On behalf of all authors, the corresponding author states that there is no conflict of interest concerning the research, authorship and publication of this article.

References

- ACI 440.2 R-17. (2017). *Guide for the design and construction of externally bonded FRP systems for strengthening concrete structures*. American Concrete Institute: American Concrete Institute.
- Adhikary, B. B., & Mutsuyoshi, H. (2004). Behavior of concrete beams strengthened in shear with carbon-fiber sheets. *Journal of Composites for Construction*, 8(3), 258–264. [https://doi.org/10.1061/\(ASCE\)1090-0268\(2004\)8:3\(258\)](https://doi.org/10.1061/(ASCE)1090-0268(2004)8:3(258))
- Al-Akhras, N. M., Jamal Shannag, M., & Malkawi, A. B. (2016). Evaluation of shear-deficient lightweight RC beams retrofitted with adhesively bonded CFRP sheets. *European Journal of Environmental and Civil Engineering*, 20(8), 899–913. <https://doi.org/10.1080/19648189.2015.1084383>
- Alam, M. A., & Al Riyami, K. (2018). Shear strengthening of reinforced concrete beam using natural fibre reinforced polymer laminates. *Construction and Building Materials*, 162, 683–696. <https://doi.org/10.1016/j.conbuildmat.2017.12.011>
- Allam, S. M., & Ebeido, T. I. (2003). Retrofitting of RC beams predamaged in shear using CFRP sheets. *Alexandria Engineering Journal*, 42(1), 87–101.
- Al-Sulaimani, G. J., Sharif, A., Basunbul, I. A., Baluch, M. H., & Ghalib, B. N. (1994). Shear repair for reinforced concrete by fiber-glass plate bonding. *ACI Structural Journal*, 91(4), 458–464. <https://doi.org/10.14359/4153>
- AS 5100.8. (2017). *Bridge design rehabilitation and strengthening of existing bridges*. Sydney: Standards Australia.
- Azam, R., Soudki, K., West, J. S., & Noël, M. (2017). Strengthening of shear-critical RC beams: Alternatives to externally bonded CFRP sheets. *Construction and Building Materials*, 151, 494–503. <https://doi.org/10.1016/j.conbuildmat.2017.06.106>
- Badaoui, M., Bourahla, N., & Bensaïbi, M. (2019). Estimation of accidental eccentricities for multi-storey buildings using artificial neural networks. *Asian Journal of Civil Engineering*, 20, 703–711. <https://doi.org/10.1007/s42107-019-00137-x>
- Badawy, M. (2020). A hybrid approach for a cost estimate of residential buildings in Egypt at the early stage. *Asian Journal of Civil Engineering*, 21, 763–774. <https://doi.org/10.1007/s42107-020-00237-z>
- Barros, J., & Dias, S. (2003). Shear strengthening of reinforced concrete beams with CFRP laminate strips of CFRP. In *International Conference Composites in Constructions (CCC2003)*, pp. 289–294. <https://doi.org/10.1680/macrc.2008.62.1.65>
- Beber, A. J., & Filho Campos, A. (2005). CFRP composites on the shear strengthening of reinforced concrete beams. *Revista Ibracon de Estruturas*, 1(2), 127–143.
- Bukhari, I. A., Vollum, R. L., Ahmad, S., & Sagaseta, J. (2010). Shear strengthening of reinforced concrete beams with CFRP. *Magazine of Concrete Research*, 62(1), 65–77. <https://doi.org/10.1680/macrc.2008.62.1.65>
- Bukhari, I. A., Vollum, R., Ahmad, S., & Sagaseta, J. (2013). Shear strengthening of short span reinforced concrete beams with CFRP sheets. *Arabian Journal for Science and Engineering*, 38(3), 523–536. <https://doi.org/10.1007/s13369-012-0333-z>
- Chaallal, O., Nollet, M.-J., & Perraton, D. (1998). Shear strengthening of RC beams by externally bonded side CFRP strips. *Journal of Composites for Construction*, 2(2), 111–113. [https://doi.org/10.1061/\(ASCE\)1090-0268\(1998\)2:2\(111\)](https://doi.org/10.1061/(ASCE)1090-0268(1998)2:2(111))
- Chen, J. F., & Teng, J. G. (2003). Shear capacity of FRP-strengthened RC beams: FRP debonding. *Construction and Building Materials*, 17, 27–41.
- Chiu, S. L. (1994). Fuzzy model identification based on cluster estimation. *Journal of Intelligent and Fuzzy Systems*, 2, 267–278.
- CSA S806-12. (2012). *Design and construction of building structures with fiber reinforced polymers*. Toronto: Canadian Standards Association.
- Ebead, U., & Saeed, H. (2017). FRP/stirrups interaction of shear-strengthened beams. *Materials and Structures/Materiaux et Constructions*, 50(2), 103. <https://doi.org/10.1617/s11527-016-0973-7>
- EN 1998-3:2005. (2005). *European committee for standardization. Eurocode 8—Design of structures for earthquake resistance—part 3: Assessment and retrofitting of buildings*. Brussels: European Committee for Standardization.
- Farghal, O. A. (2012). Shear strengthening of R. C. T-beams by means of CFRP sheets. *Journal of Engineering Sciences*, 40(5), 1293–1307.
- fib-TG 9.3. (2001). *Externally bonded FRP reinforcement for RC structures*. Lausanne: International Federation for Structural Concrete.

- Golnargesi, S., Shariatmadar, H., & Razavi, H. M. (2018). Seismic control of buildings with active tuned mass damper through interval type-2 fuzzy logic controller including soil–structure interaction. *Asian Journal of Civil Engineering*, 19(2), 177–188. <https://doi.org/10.1007/s42107-018-0016-5>
- Grande, E., Imbimbo, M., & Rasulo, A. (2009). Effect of transverse steel on the response of RC beams strengthened in shear by FRP: Experimental study. *Journal of Composites for Construction*, 13(5), 405–414. [https://doi.org/10.1061/\(ASCE\)1090-0268\(2009\)13:5\(405\)](https://doi.org/10.1061/(ASCE)1090-0268(2009)13:5(405))
- Jalal, M., Arabali, P., Grasley, Z., & Bullard, J. W. (2020). Application of adaptive neuro-fuzzy inference system for strength prediction of rubberized concrete containing silica fume and zeolite. *Proceedings of the Institution of Mechanical Engineers Part L Journal of Materials: Design and Applications*, 234(3), 438–451. <https://doi.org/10.1177/1464420719890370>
- Jang, J. S. (1993). ANFIS: Adaptive-network-based fuzzy inference system. *IEEE Transactions On Systems Man And Cybernetics*, 23(3), 665–685. <https://doi.org/10.1093/nq/184.1.17>
- Kar, S., & Biswal, K. C. (2020a). Shear strengthening of RC beams with basalt fiber reinforced polymer (BFRP) composites. *Advances in Concrete Construction*, 10(2), 93–104. <https://doi.org/10.12989/acc.2020.10.2.093>
- Kar, S., & Biswal, K. C. (2020b). FRP shear contribution prediction for U-wrapped RC T-beams using a soft computing tool. *Structures*, 27, 1093–1104. <https://doi.org/10.1016/j.istruc.2020.06.023>
- Kar, S., & Biswal, K. C. (2020c). Shear strengthening of reinforced concrete T-Beams by using fiber-reinforced polymer composites: A data analysis. *Arabian Journal for Science and Engineering*. <https://doi.org/10.1007/s13369-020-04412-x>
- Kar, S., Pandit, A. R., & Biswal, K. C. (2020). Prediction of FRP shear contribution for wrapped shear deficient RC beams using adaptive neuro-fuzzy inference system (ANFIS). *Structures*, 23, 702–717. <https://doi.org/10.1016/j.istruc.2019.10.022>
- Kawady, T. A., Sowilam, G. M., & Shalwala, R. (2020). Improved distance relaying for double-circuit lines using adaptive neuro-fuzzy inference system. *Arabian Journal for Science and Engineering*, 45(3), 1969–1984. <https://doi.org/10.1007/s13369-020-04369-x>
- Khalifa, A., Gold, W. J., Nanni, A., & Abdel Aziz, M. I. (1998). Contribution of externally bonded FRP to shear capacity of RC flexural members. *Journal of Composites for Construction*, 2(4), 195–202. [https://doi.org/10.1061/\(ASCE\)1090-0268\(1998\)2:4\(195\)](https://doi.org/10.1061/(ASCE)1090-0268(1998)2:4(195))
- Khalifa, A., & Nanni, A. (2000). Improving shear capacity of existing RC T-section beams using CFRP composites. *Cement and Concrete Composites*, 22, 165–174.
- Khoshevisan, B., Rafiee, S., Omid, M., Mousazadeh, H., & Clark, S. (2014). Environmental impact assessment of tomato and cucumber cultivation in greenhouses using life cycle assessment and adaptive neuro-fuzzy inference system. *Journal of Cleaner Production*, 73, 183–192. <https://doi.org/10.1016/j.jclepro.2013.09.057>
- Kibria, B. M. G., Ahmed, F., Ahsan, R., & Ansary, M. A. (2020). Experimental investigation on behavior of reinforced concrete interior beam column joints retrofitted with fiber reinforced polymers. *Asian Journal of Civil Engineering*, 21(1), 157–171. <https://doi.org/10.1007/s42107-019-00204-3>
- Kreinovich, V., Quintana, C., & Reznik, L. (1992). Gaussian membership functions are most adequate in representing uncertainty in measurements. In *Proceedings of NAFIPS*, pp. 1–7
- Li, A., Diagana, C., & Delmas, Y. (2001). CRFP contribution to shear capacity of strengthened RC beams. *Engineering Structures*, 23(10), 1212–1220. [https://doi.org/10.1016/S0141-0296\(01\)00035-9](https://doi.org/10.1016/S0141-0296(01)00035-9)
- Lim, D. H. (2010). Shear behaviour of RC beams strengthened with NSM and EB CFRP strips. *Magazine of Concrete Research*, 62(3), 211–220. <https://doi.org/10.1680/macrc.2010.62.3.211>
- Mofidi, A., & Chaallal, O. (2011). Shear strengthening of RC beams with EB FRP: Influencing factors and conceptual debonding model. *Journal of Composites for Construction*, 15(1), 62–74. [https://doi.org/10.1061/\(ASCE\)CC.1943-5614.0000153](https://doi.org/10.1061/(ASCE)CC.1943-5614.0000153)
- Monti, G., & Liotta, M. (2007). Tests and design equations for FRP-strengthening in shear. *Construction and Building Materials*, 21(4), 799–809. <https://doi.org/10.1016/j.conbuildmat.2006.06.023>
- Mostofinejad, D., Hosseini, S. A., & Razavi, S. B. (2016). Influence of different bonding and wrapping techniques on performance of beams strengthened in shear using CFRP reinforcement. *Construction and Building Materials*, 116, 310–320. <https://doi.org/10.1016/j.conbuildmat.2016.04.113>
- Naderpour, H., & Alavi, S. A. (2017). A proposed model to estimate shear contribution of FRP in strengthened RC beams in terms of adaptive neuro-fuzzy inference system. *Composite Structures*, 170, 215–227. <https://doi.org/10.1016/j.compstruct.2017.03.028>
- Naderpour, H., & Mirrashid, M. (2020). Proposed soft computing models for moment capacity prediction of reinforced concrete columns. *Soft Computing*. <https://doi.org/10.1007/s00500-019-04634-8>
- Nguyen, Q., Behroyan, I., Rezakazemi, M., & Shirazian, S. (2020). Fluid velocity prediction inside bubble column reactor using ANFIS algorithm based on CFD input data. *Arabian Journal for Science and Engineering*. <https://doi.org/10.1007/s13369-020-04611-6>
- Nikopour, H., & Nehdi, M. (2011). Shear repair of RC beams using epoxy injection and hybrid external FRP. *Materials and Structures*, 44(10), 1865–1877. <https://doi.org/10.1617/s11527-011-9743-8>
- Norris, T., Saadatmanesh, H., & Ehsani, M. R. (1997). Shear and flexural strengthening of R/C beams with carbon fiber sheets. *Journal of Structural Engineering*, 123(7), 903–911. [https://doi.org/10.1061/\(ASCE\)0733-9445\(1997\)123:7\(903\)](https://doi.org/10.1061/(ASCE)0733-9445(1997)123:7(903))
- Obaidat, Y. T., Heyden, S., Dahlblom, O., Abu-Farsakh, G., & Abdel-Jawad, Y. (2011). Retrofitting of reinforced concrete beams using composite laminates. *Construction and Building Materials*, 25(2), 591–597. <https://doi.org/10.1016/j.conbuildmat.2010.06.082>
- Panda, K. C., Bhattacharyya, S. K., & Barai, S. V. (2011). Shear strengthening of RC T-beams with externally side bonded GFRP sheet. *Journal of Reinforced Plastics and Composites*, 30(13), 1139–1154. <https://doi.org/10.1177/0731684411417202>
- Panda, K. C., Bhattacharyya, S. K., & Barai, S. V. (2013a). Effect of transverse steel on the performance of RC T-beams strengthened in shear zone with GFRP sheet. *Construction and Building Materials*, 41, 79–90. <https://doi.org/10.1016/j.conbuildmat.2012.11.098>
- Panda, K. C., Bhattacharyya, S. K., & Barai, S. V. (2013b). Shear strengthening effect by bonded GFRP strips and transverse steel on RC T-beams. *Structural Engineering and Mechanics*, 47(1), 75–98. <https://doi.org/10.12989/sem.2013.47.1.075>
- Pandit, M., Chaudhary, V., Dubey, H. M., & Panigrahi, B. K. (2015). Multi-period wind integrated optimal dispatch using series PSO-DE with time-varying Gaussian membership function based fuzzy selection. *International Journal of Electrical Power and Energy Systems*, 73, 259–272. <https://doi.org/10.1016/j.ijepe.2015.05.017>
- Panigrahi, A. K., Biswal, K. C., & Barik, M. R. (2014). Strengthening of shear deficient RC T-beams with externally bonded GFRP sheets. *Construction and Building Materials*, 57, 81–91. <https://doi.org/10.1016/j.conbuildmat.2014.01.076>
- Panjehpour, M., Abdullah, A., Ali, A., Voo, Y. L., & Aznieta, F. N. (2014). Effective compressive strength of strut in CFRP-strengthened reinforced concrete deep beams following ACI 318–11. *Computers and Concrete*, 13(1), 135–165.

- Pellegrino, C., & Modena, C. (2002). Fiber reinforced polymer shear strengthening of reinforced concrete beams with transverse steel reinforcement. *Journal of Composites for Construction*, 6(2), 104–111. [https://doi.org/10.1061/\(ASCE\)1090-0268\(2002\)6:2\(104\)](https://doi.org/10.1061/(ASCE)1090-0268(2002)6:2(104))
- Pham, T. M., & Hao, H. (2016). Impact behavior of FRP-strengthened RC beams without Stirrups. *Journal of Composites for Construction*, 20(4), 04016011. [https://doi.org/10.1061/\(asce\)cc.1943-5614.0000671](https://doi.org/10.1061/(asce)cc.1943-5614.0000671)
- Safa, M., Shariati, M., Ibrahim, Z., Toghroli, A., Baharom, S. B., Nor, N. M., & Petkovic, D. (2016). Potential of adaptive neuro fuzzy inference system for evaluating the factors affecting steel-concrete composite beam's shear strength. *Steel and Composite Structures*, 21(3), 679–688. <https://doi.org/10.12989/scs.2016.21.3.679>
- Shariati, M., Mafipour, M. S., Haido, J. H., Yousif, S. T., Toghroli, A., Trung, N. T., & Shariati, A. (2020). Identification of the most influencing parameters on the properties of corroded concrete beams using an Adaptive Neuro-Fuzzy Inference System (ANFIS). *Computers and Concrete*, 34(1), 155–170.
- Sharifi, Y., Moghbeli, A., Hosseinpour, M., & Sharifi, H. (2019). Neural networks for lateral torsional buckling strength assessment of cellular steel I-beams. *Advances in Structural Engineering*, 22(9), 2192–2202. <https://doi.org/10.1177/1369433219836176>
- Singh, V. K., Kumari, A., & Yadav, A. K. S. (2013). Approximations of fuzzy systems. *Indonesian Journal of Electrical Engineering and Informatics (IJEEI)*, 1(1), 14–20. <https://doi.org/10.11591/ijeei.v1i1.52>
- Tan, Y., Shuai, C., Jiao, L., & Shen, L. (2017). An adaptive neuro-fuzzy inference system (ANFIS) approach for measuring country sustainability performance. *Environmental Impact Assessment Review*, 65(April), 29–40. <https://doi.org/10.1016/j.eiar.2017.04.004>
- Tetta, Z. C., Koutas, L. N., & Bournas, D. A. (2015). Textile-reinforced mortar (TRM) versus fiber-reinforced polymers (FRP) in shear strengthening of concrete beams. *Composites Part B Engineering*, 77, 338–348. <https://doi.org/10.1016/j.compositesb.2015.03.055>
- TR 55. (2012). Design guidance for strengthening concrete structures using fibre composite materials. The concrete society Technical report TR55.
- Triantafillou, T. C. (1998). Shear strengthening of reinforced concrete beams using epoxy-bonded FRP composites. *ACI Structural Journal*, 95(2), 107–115. <https://doi.org/10.3109/01676830903538664>
- Vasileva-Stojanovska, T., Vasileva, M., Malinovski, T., & Trajkovik, V. (2015). An ANFIS model of quality of experience prediction in education. *Applied Soft Computing Journal*, 34, 129–138. <https://doi.org/10.1016/j.asoc.2015.04.047>
- Zadeh, L. A. (1965). Fuzzy Sets. *Information and Control*, 8, 338–353. <https://doi.org/10.1109/2.53>
- Zhang, Z., & Hsu, C.-T.T. (2005). Shear strengthening of reinforced concrete beams using carbon-fiber-reinforced polymer laminates. *Journal of Composites for Construction*, 9(2), 158–169. [https://doi.org/10.1061/\(ASCE\)1090-0268\(2005\)9:2\(158\)](https://doi.org/10.1061/(ASCE)1090-0268(2005)9:2(158))
- Zhang, Z., Hsu, C. T. T., & Moren, J. (2004). Shear strengthening of reinforced concrete beams using carbon-fiber-reinforced polymer laminates. *Journal of Composites for Construction*, 8(5), 403–414. [https://doi.org/10.1061/\(ASCE\)1090-0268\(2004\)8:5\(403\)](https://doi.org/10.1061/(ASCE)1090-0268(2004)8:5(403))

Publisher's Note Springer Nature remains neutral with regard to jurisdictional claims in published maps and institutional affiliations.